analytical chemistry

Article

Cite This: Anal. Chem. 2017, 89, 13502−13507

pubs.acs.org/ac

Simultaneous Analysis of a Non-Lipidated Protein and Its Lipidated Counterpart: Enabling Quantitative Investigation of Protein Lipidation's Impact on Cellular Regulation

Agnesa Shala-Lawrence,[†,#] Melanie J. Blanden,[‡,#] Svetlana M. Krylova,[†] Soumyashree A. Gangopadhyay,[‡] Stanislav S. Beloborodov,[†] James L. Hougland,[*,‡] and Sergey N. Krylov[*,†]

[†]Department of Chemistry and Centre for Research on Biomolecular Interactions, York University, Toronto, Ontario M3J 1P3, Canada

[‡]Department of Chemistry, Syracuse University, Syracuse, New York 13244, United States

Supporting Information

ABSTRACT: Here, we introduce protein−lipidation quantitation (PLQ)—the first method for quantitative analysis of both a substrate and a product of protein lipidation in a biologically relevant context. Such analysis is required to study roles of protein lipidation in cellular regulation. In PLQ, the substrate is fused with a fluorescent protein to facilitate quantitative detection of both the nonlipidated substrate and the lipidated product. When expressed in cells with endogenous lipidation activity, the substrate is intracellularly lipidated. Following cell lysis and sampling crude cell lysate for analysis, the substrate and the product are separated by surfactant-mediated capillary electrophoresis (CE) and quantitated by integrating fluorescence intensity over respective CE peaks. In this work, we prove PLQ in principle and demonstrate its robustness to changes in structures of the substrate and lipid donor. Finally, PLQ analysis confirms a hypothesized link between a mutation in p53 and cellular prenylation activity.

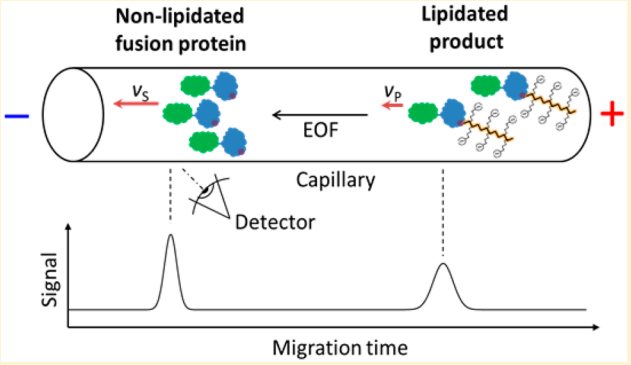

Transduction of external and internal signals is involved in regulation of major cellular processes, such as cell proliferation, differentiation, and apoptosis.[1−3] Posttranslational modifications (PTMs) of proteins are, in turn, a major means of signal transduction in cells.[4] During signal transduction, an upstream signal often modulates the activity of an enzyme responsible for conversion of an unmodified protein substrate (S) to the modified protein product (P) (Figure 1). Understanding how the balance between S and P affects cellular response requires simultaneous measurement of amounts of S and P proteins upon PTMs.

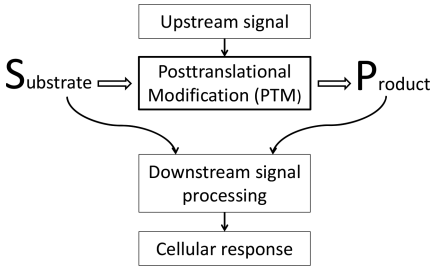

Figure 1. Schematic illustration of the role of protein PTMs in cellular signal processing.

Lipidation PTMs have received less study than other modification classes such as phosphorylation or acetylation.[5] The most well-known role of protein lipidation in signal transduction is facilitation of membrane localization of a signal receptor.[6,7] Several types of protein lipidation have been identified including prenylation, palmitoylation, myristoylation, and glycophosphatidylinositol anchoring, with each differing in the length of lipid chain, requirements for the modification, subsequent processing, and its effect on the cell.[8−16] A quantitative understanding of the role played by protein lipidation in cellular biology requires a method that can simultaneously measure the amounts of a nonlipidated substrate protein and its lipidated product (see Figure 1). A suitable method must satisfy 3 major requirements. First, it should be able to detect both S and P with a known relation between their signal/concentration ratios to allow their accurate relative quantitation. Second, for the same reason, it should absolutely discriminate signals of S and P from each other. Third, it should be applicable to crude cell lysates as any sample purification may introduce a bias toward S or P and

Received: September 20, 2017
Accepted: November 16, 2017
Published: November 16, 2017

DOI: 10.1021/acs.analchem.7b03846
Anal. Chem. 2017, 89, 13502−13507

affect the accuracy of measurements. Most available methods for studying lipidation do not satisfy requirement 1 as they rely on detecting a labeled lipid moiety, and are, hence, capable of detecting only P, but not S.[17−28] A few methods that can detect both S and P lack capabilities for accurate quantitation as they do not satisfy requirement 2.[29−33] Thus, there is no current method that satisfies all 3 requirements.

To address this challenge, we introduce protein−lipidation quantitation (PLQ)—a new bioanalytical approach that satisfies these 3 requirements for analysis of protein lipidation in cell-based models. In PLQ, the lipidation substrate is genetically fused with a fluorescent protein tag to enable sensitive and quantitative detection of both S and P. The fusion substrate is expressed in cells where it is subject to lipidation by endogenous enzymes, leading to a mixed cellular population of S and P. Following cell lysis, P is physically separated from S in a column format without a stationary phase to facilitate analysis of crude cell lysate. Finally, the concentrations of S and P in the cell lysate are accurately quantitated via fluorescence integration of signal from the fluorescent protein tag. We use the term of PLQ for both the general approach described above and for its practical implementation described below.

The practical realization of PLQ requires fluorescent protein substrates and a suitable method for separation of P from S. We and others have utilized fluorescently tagged fusion protein substrates for monitoring protein prenylation and demonstrated their intracellular modification via product localization to cellular membranes.[25,34−41] To resolve and quantitatively detect S and P directly from crude cell lysate, we turned to capillary electrophoresis (CE) which has better resolving power and detection limit than 2 other stationary-phase-free column separation platforms: hydrodynamic chromatography, and field flow fractionation.[42−44] Advantageously in CE, both positively- and negatively charged species can reach the detector if separation is carried out in the presence of a strong electroosmotic flow (EOF). Moreover, separation of two analytes with similar charge-to-size ratios can be achieved by adding a pseudostationary phase to the run buffer. For example, addition of a water-soluble (or suspended) molecule (or particle) can introduce a shift in an analyte's electrophoretic mobility through preferential analyte binding.[45,46] The present work was inspired by an insight that an ionic surfactant could potentially serve as a pseudostationary phase for separation of P from S by binding to the lipid moiety on P (Figure 2). This approach is similar to previous micellar CE separation of small prenylated peptides from their nonprenylated counterparts.[47,48] However, its applicability to proteins is not obvious since: (i) proteins are too large to be solubilized by micelles, but hydrophobic moieties on both S and P can interact with the surfactant, suppressing differential mobility introduced by surfactant's binding to the lipid on P and (ii) proteins can be denatured by SDS which would lead to accessibility of internal hydrophobic moieties for SDS and further suppress the differential mobility.

EXPERIMENTAL SECTION

Materials and Chemicals. Fused silica capillary (75 μm inner diameter, 360 μm outer diameter) was purchased from Molex (Phoenix, AZ). All chemicals were obtained from Sigma-Aldrich (Oakville, ON, Canada) unless otherwise stated. Disodium Tetrborate (borax) was purchased from EMD (Toronto, ON, Canada). All solutions were made using deionized Mili-Q water filtered through 0.22 μm Millipore filter (Millipore, Nepean, ON, Canada).

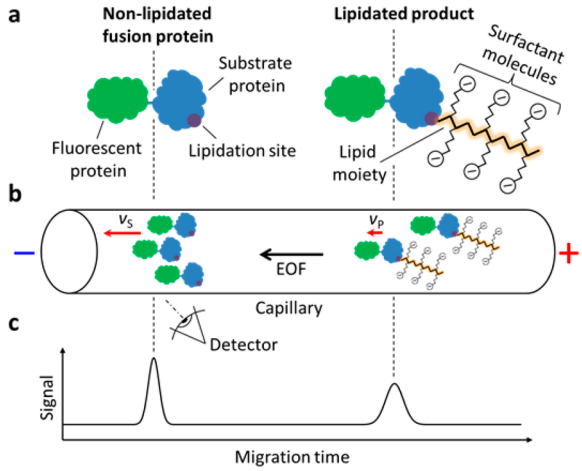

Figure 2. Conceptual illustration of PLQ. (a) Nonlipidated fusion protein (S) and its lipidated product (P) with an anionic (for example) surfactant bound to a lipid moiety of the latter. (b) S and P in a capillary filled with the surfactant in the run buffer (not shown), an electric field and EOF. Both S and P are propelled toward the cathode by EOF, however, the charge added to P by the lipid-bound surfactant makes its resulting velocity (v_P) different (smaller in our example) than that of S (v_S). (c) Schematic dependence of fluorescence signal on time for the separated S and P. Areas of peaks are proportional to the respective concentrations.

Preparation of the Proteins. The eGFP-GCVDS fusion protein was expressed in *Escherichia coli* (*E. coli*) and was used either as a His-tag affinity-purified protein or as a component of a crude bacterial lysate. To obtain the farnesylated product, purified eGFP-GCVDS or a crude cell lysate containing eGFP-GCVDS was incubated with purified recombinant FTase and FPP using established protocols.[49−51] The expression, purification and lipidation of eGFP-GCVLL and TagRFP-GCVDS fusion proteins were conducted in a similar way (see Supporting Information). TagRFP-Hras-CVLL and eGFP-Hras were expressed and lipidated in HEK293 and MDA-231shp53 cells, respectively (see Supporting Information). Prior to the CE experiments, HEK293 and MDA-231 shp53 cells were centrifuged for 2 min at ∼13000 × g (Eppendorf 5417R centrifuge with F45−30−11 rotor (Fisher scientific, PA, USA)) at 4 °C and the supernatant was collected. The obtained supernatant as well as purified proteins were diluted with the sample buffer consisting of 50 mM HEPES sodium salt (NaHEPPSO), 10 mM $MgCl_2$, 5 mM tris(2-carboxyethyl)-phosphine hydrochloride (TCEP), and 10 mg/mL bovine serum albumin (BSA) at pH 7.8. The BSA was added to reduce adsorption of the proteins onto capillary surface.

Capillary Electrophoresis. CE experiments were carried out with MDQ-PACE instrument (Sciex, formerly Beckman-Coulter, Caledon, ON, Canada) using laser-induced fluorescence (LIF) detection with excitation at 488 nm and emission at 520 and 610 nm for the detection of eGFP and TagRFP derivatives, respectively. Fused silica capillaries with total length of 84 cm were preconditioned by sequential washing with 100 mM HCl, 100 mM NaOH, Milli-Q water and run buffer each for 2 min at 30 psi (206.84 kPa). In a beginning of each experiment capillaries were rinsed with each of the following solutions: 100 mM HCl, 100 mM NaOH Milli-Q water for 2 min at 30 psi (206.84 kPa) and with run buffer for 2 min at 40

DOI: 10.1021/acs.analchem.7b03846
Anal. Chem. 2017, 89, 13502−13507

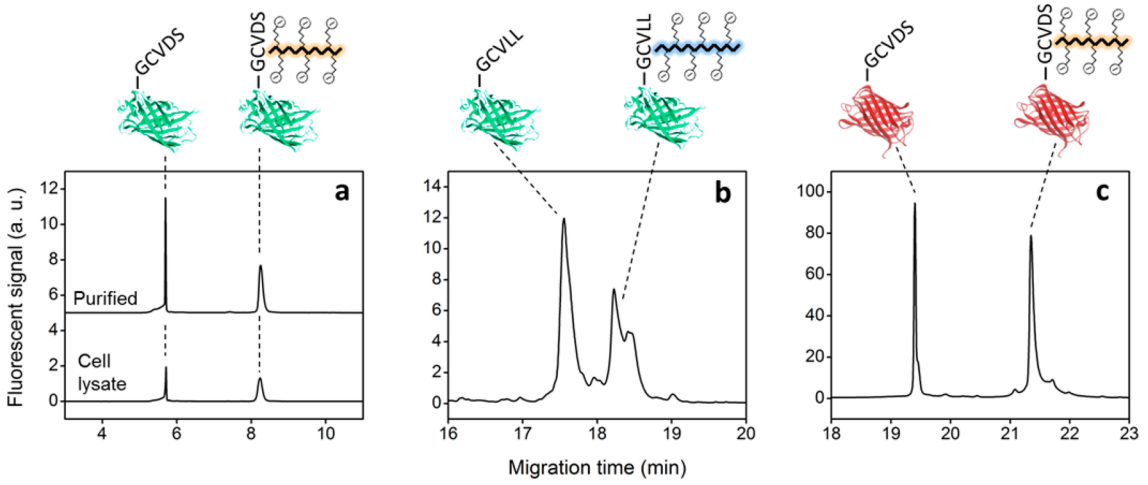

Figure 3. PLQ separation of various prenylation constructs. (a) S, eGFP-GCVDS; P; farnesylated eGFP-GCVDS. Top trace, purified S and P in 50 mM NaHEPPSO pH 7.8 and 5 mM TCEP; bottom trace, S and P present in the crude bacterial cell lysate. The run buffer was 25 mM Borax, 20 mM SDS at pH 9.2. (b) S, eGFP-GCVLL; P, geranylgeranylated eGFP-GCVLL. Purified S and P were in 50 mM NaHEPPSO pH 7.8 and 5 mM TCEP; run buffer was 25 mM Borax, 20 mM SDS at pH 9.2 (c) S, TagRFP-GCVDS; P, farnesylated TagRFP-GCVDS. Purified S and P were in 50 mM Na-HEPPSO pH 7.8 and 5 mM TCEP; run buffer was 25 mM sodium tetraborate, 20 mM SDS at pH 10.0. Results of separate CE analyses of all substrates and their prenylated products are shown in Figure S4.

psi (275.79 kPa). The samples were injected into the capillary by 1 psi (6.89 kPa) pressure pulse of 28 s. Electrophoretic separation was carried out with a positive electrode at the injection end of the capillary, with electric field strength of 297 V/cm.

RESULTS AND DISCUSSION

For the initial validation of the proposed practical realization of PLQ, we chose enhanced green fluorescent protein (eGFP) fused with a GCVDS peptide to permit modification by protein farnesyltransferase (FTase) using a farnesyl diphosphate (FPP) lipid donor. The GCVDS motif was chosen as part of an ongoing study into a bioorthogonal substrate-enzyme relationship in which a mutant FTase lipidates a noncanonical prenylation motif.[49]

A mixture of the purified eGFP-GCVDS and its farnesylated product was used in the surfactant-testing experiments with peak assignments by single-component injection. Upon initial testing, nonionic surfactants did not introduce noticeable mobility shift. The choice of ionic surfactants was limited to anionic compounds as cationic surfactants would bind to the negatively charged inner surface of fused-silica capillary and suppress EOF, which was undesirable. We began tests of anionic surfactants with sodium dodecyl sulfate (SDS) because it has been previously used in CE as a pseudostationary phase for small-molecule separation.[52] The concentration of SDS was kept well below that typically used for protein denaturation (~70 mM SDS, combined with sample heating to 100 °C and addition of reducing agents in denaturing protein analyses). Analysis in the presence of SDS yielded detectable separation of farnesylated and nonfarnesylated eGFP-GCVDS. The farnesylated product migrated slower in agreement with our model in which a negatively charged surfactant should slow down migration of P during PLQ analysis (Figure 2).

To satisfy requirement 2 (absolute discrimination between signals from S and P), the composition of the run buffer was optimized with regards to SDS concentration, pH, and ionic strength to achieve maximum resolution between peaks of S and P (see Supporting Information). The optimized conditions (20 mM SDS, 25 mM sodium tetraborate, pH 9.2) facilitated baseline separation of farnesylated and nonfarnesylated eGFP-GCVDS (Figure 3a). Analyses of electrophoretic mobilities of S and P in the optimum SDS-containing buffer allowed us to estimate the number of SDS molecules bound to a farnesyl moiety to be 4 to 6 (see Supporting Information). To test if SDS-mediated separation satisfies requirement 3, which deals with suitability for analysis of crude cell lysate, we sampled the crude bacterial cell lysate containing both eGFP-GCVDS and its farnesylated product. We observed high-quality separation undistinguishable from that of purified S and P (Figure 3a), thus, confirming satisfaction of requirement 3. Addressing requirement 1, we found that farnesylation did not affect fluorescence of eGFP-GCVDS, and the presence of 20 mM SDS (optimal concentration) did not change fluorescence from eGFP-GCVDS above normal experiment-to-experiment variation. These results confirmed that signal/concentration ratios for both S and P were similar. This allows simple quantitation of S and P concentrations in the sample based on areas of the corresponding peaks, with absolute quantitation possible through use of an internal standard.

After proving that CE-based PLQ satisfies requirements 1−3 for farnesylation of eGFP-GCVDS, we tested assay robustness with regards to changes in structures of the lipid donor and fusion protein (consisting of the substrate protein and fluorescent protein). First, we explored a different lipid donor by replacing FPP with geranylgeranyl diphosphate (GGPP). The substrate of lipidation was eGFP fused with the GCVLL peptide sequence; protein geranylgeranyltransferase type I (GGTase-I) was used to geranylgeranylate eGFP-GCVLL. Separation was achieved for nongeranylgeranylated and geranylgeranylated eGFP-GCVLL without reoptimization of separation conditions (Figure 3b). Second, we replaced eGFP with red fluorescent protein (TagRFP) while maintaining the GCVDS farnesylation motif.[49] Reoptimization of pH was conducted, and maximum resolution between the S and P forms of TagRFP-GCVDS was achieved at pH 10.0 (Figure 3c). The need for pH reoptimization indirectly suggests that the fluorescent protein interacts with SDS and the extent of this

DOI: 10.1021/acs.analchem.7b03846
Anal. Chem. 2017, 89, 13502−13507

interaction can be decreased by changing buffer pH. Third, we replaced the short peptide (GCVDS or GCVLL) with a full-length human HRas protein which was fused with eGFP and expressed in HEK293 cells (Figure 4, upper curve). To

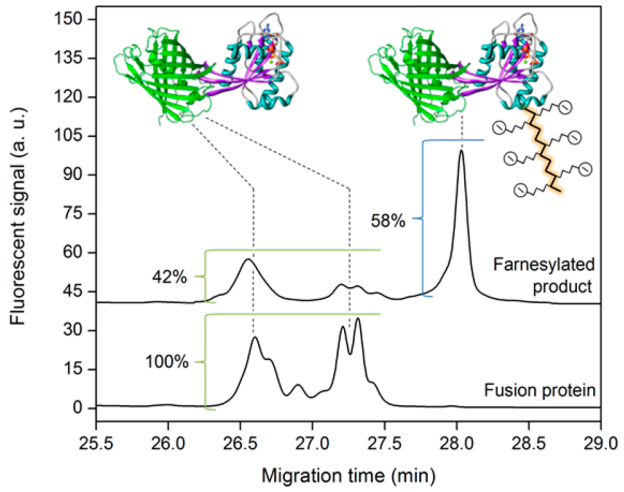

Figure 4. PLQ analysis of endogenous farnesylation of eGFP-HRas fusion protein. The lower curve corresponds to sampling cell lysate prepared from HEK293 cells grown in the presence of a FTase inhibitor and shows peaks generated by the nonfarnesylated eGFP-HRas. The upper trace corresponds to sampling cell lysate prepared from HEK293 cells grown without inhibition of FTase and shows the peak of farnesylated eGFP-HRas at the right and peaks of nonfarnesylated eGFP-HRas at the left. The run buffer was 50 mM sodium tetraborate, 20 mM SDS at pH 9.2. Percentile shows concentrations of nonfarnesylated and farnesylated eGFP-HRas calculated from the areas of corresponding peaks.

generate the unmodified form of eGFP-HRas in the cellular context, transfected cells were treated with an FTase inhibitor (tipifarnib) to block cellular farnesylation activity.[53,54] Sampling the cell lysate prepared from the FTase-inhibited cells revealed 2 prominent peaks (Figure 4, lower curve). However, sampling the cell lysate prepared from cells grown without the FTase inhibitor to allow protein farnesylation by endogenous FTase showed a new peak corresponding to the farnesylated protein and the decreased 2 peaks associated with the substrate (Figure 4, upper curve). Separation of S from P for this larger size fusion protein (54 kDa) required reoptimization of conditions; the optimum separation was achieved at a higher ionic strength of the SDS-containing run buffer: 50 mM instead of 25 mM sodium tetraborate. Quantitative features of PLQ allowed us to determine the level of lipidated substrate in the presence of inhibitor being below the limit of detection while in the absence of inhibitor it grew to 58%, which demonstrates the ability of PLQ analysis to accurately determine the fraction of a given protein within a cell that undergoes lipid modification.

We found that prenylation did not affect the quantum yield of the fluorescent proteins. Therefore, PLQ introduces no bias toward measured S/P ratios. The limit of detection and the dynamic range of detection of the PLQ method are solely defined by the characteristics of CE detection. A commercial instrument used in this study supports an LOD of below 10 pM and a linear dynamic range of at least 3 orders of magnitude. Importantly, all quantitative characteristics are retained in the analysis of crude cell lysates since the cell debris is fully separated from the fluorescent analytes and does not affect detection. Moreover, the quantitative characteristics are independent of the substrate protein nature because they are defined by the fluorescent properties of GFP or RFP which do not change significantly upon fusion to a substrate protein and, in addition, are little affected by substrate lipidation

We confirmed that PLQ satisfied requirements 1−3 for the three above-described modifications, proving that our method was robust to changes in lipid donor, fluorescent protein, and lipid acceptor with minimal reoptimization. These findings emphasize the practicality of PLQ approach and suggest that PLQ implementation with a fluorescent fusion protein and SDS-mediated CE as a stationary-phase-free column separation method is a robust approach for investigating protein lipidation in biologically relevant contexts.

To demonstrate the utility of PLQ in addressing complex biological questions, we have applied it to determine the impact of p53 mutation on protein prenylation in a breast cancer cell line. It was recently reported the presence of mutated p53 tumor suppression gene in the MDA-231 breast cancer cell line is associated with prenylation-dependent changes in cell morphology and growth.[55] In this work, the presence of the mutated p53 gene is proposed to impact prenylation activity in breast cancer cells.[55] Our ability to separate nonprenylated and prenylated proteins provides an ideal approach to directly probe the impact of the presence of mutated p53 on cellular protein prenylation.

To examine the influence of a p53 mutation on prenylation activity, we used the MDA-231shp53 cell line which has been engineered to express a doxycycline (Dox)-inducible shRNA silencing of the endogenous mutant p53 gene.[55] MDA-231shp53 cells were transfected with an RFP-tagged substrate for GGTase-I (Supporting Information) in the presence and absence of Dox. Crude lysates from these cells were analyzed by PLQ using conditions optimized for TagRFP-containing fusion protein substrates; the results are shown in Figure 5. In the presence of Dox (when mutated p53 was silenced), the peak of the geranylgeranylated form of the TagRFP substrate was below the limit of detection, confirming that less than 5% of the substrate was prenylated. In contrast, in the absence of Dox (when mutated p53 was expressed), the peak corresponding to the geranylgeranylated product of TagRFP indicated that more than 95% of the substrate was prenylated. Control experiments using HEK293 cells indicate that Dox treatment alone does not influence protein geranylgeranylation in the absence of the mutated p53 gene (Figure S3) This study demonstrates that silencing of mutant p53 expression exhibits a functional effect on cellular GGTase-I activity similar to that of direct inhibition of cellular FTase activity by FTase inhibitor treatment (Figure 4). These findings support the model wherein p53 mutations lead to altered cellular prenylation activity and suggests that altered protein prenylation may play a direct role in cellular changes involved in oncogenic transformation.

CONCLUSION

To conclude, we proposed a general approach for simultaneous analysis of substrate and product of protein lipidation and demonstrated its practical implementation with GFP- and RFP-fusion proteins as substrates and SDS-mediated CE as a stationary-phase-free column separation method. We showed that this analysis is applicable to crude cell lysates without any sample purification, which further contributes to the analysis accuracy. Finally, we demonstrated that our approach can facilitate experiments addressing biological question involving

DOI: 10.1021/acs.analchem.7b03846
Anal. Chem. 2017, 89, 13502−13507

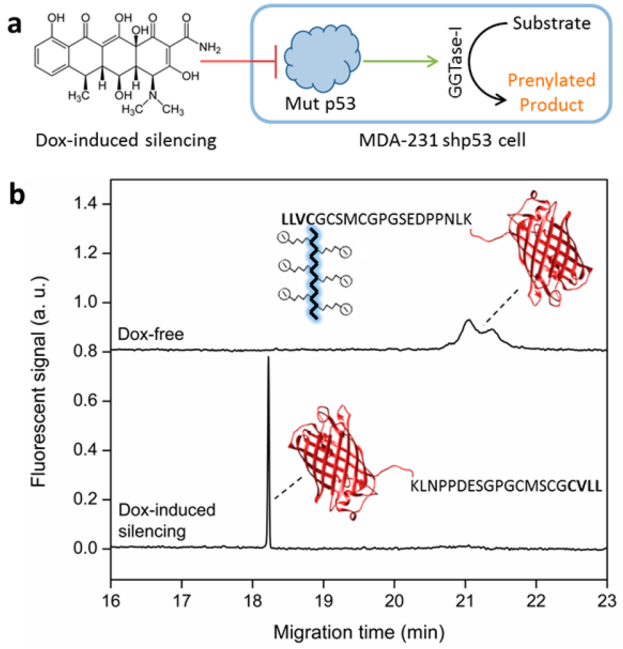

Figure 5. PLQ analysis of the impact of p53 mutation on cellular prenylation activity. (a) Schematic representation of cellular model for testing the impact of mutant p53 expression on protein prenylation. (b) PLQ analysis of cell lysates prepared from cells grown in the absence (top trace) and presence (bottom trace) of Dox.

protein lipidation. PLQ provides a powerful complement to fluorescence microscopy for studying protein lipidation within the cell. The latter can be used to study the change in protein cellular localization upon lipidation while the former can accurately assess the extent of protein lipidation potentially at both the single-cell and cell-population scales. The combined use of PLQ and microscopy will uniquely enable researchers to identify and study proteins in which the role of lipidation is not to enhance plasma localization, for example, Ydj1p heat shock protein recently reported on by Hildebrant and co-workers.[56] In the growing field of protein lipidation, the quantitative capabilities of PLQ will allow researchers to formulate and address previously intractable quantitative questions. PLQ thus promises to become a powerful tool in studies of roles of protein lipidation in cellular regulation and biological function. This work also adds lipidation to a set of postrtranslational modifications of proteins (PEGylation, glycosylation, carbonylation, phosphorylation) for which CE analyses have been developed.[57−60]

■ ASSOCIATED CONTENT

Supporting Information

The Supporting Information is available free of charge on the ACS Publications website at DOI: 10.1021/acs.analchem.7b03846.

Experimental procedures; estimation of the number of SDS molecules per farnesylated eGFP-GCVDS; electroosmotic (μ_0) and electrophoretic (μ) mobilities of analyzed proteins; doxycycline treatment of MDA-231shp53 cells suppresses mutant p53 expression; influence of SDS concentration on separation efficiency of farnesylated and nonfarnesylated eGFP; control experiments with HEK293 cells in the absence of the mutated p53 gene; representative electropherograms for the unmodified and modified proteins (PDF)

■ AUTHOR INFORMATION

Corresponding Authors

*E-mail: hougland@syr.edu.
*E-mail: skrylov@yorku.ca.

ORCID

James L. Hougland: 0000-0003-0444-1017
Sergey N. Krylov: 0000-0003-3270-2130

Author Contributions

#A.S.-L. and M.J.B. contributed equally to the scientific work described in present manuscript

Notes

The authors declare no competing financial interest.

■ ACKNOWLEDGMENTS

This work was supported by NSERC Canada (STPGP 463455), the American Cancer Society (IRG-11-052-01), and a U.S. Department of Education GAANN Fellowship (P200A090277 to M.J.B.). We thank Mark Distefano (Univ. of Minnesota) for the gift of bacterial expression vectors, Patrick Casey (Duke Medical School) for the gift of mammalian expression vectors, and Jill Bargonetti (Hunter College/CUNY) for the gift of the MDA-231shp53 cell line.

■ REFERENCES

(1) Zuccolo, E.; Dragoni, S.; Poletto, V.; Catarsi, P.; Guido, D.; Rappa, A.; Reforgiato, M.; Lodola, F.; Lim, D.; Rosti, V.; et al. *Vasc. Pharmacol.* **2016**, *87*, 159−171.
(2) Mauro, C.; Smith, J.; Cucchi, D.; Coe, D.; Fu, H.; Bonacina, F.; Baragetti, A.; Cermenati, G.; Caruso, D.; Mitro, N.; et al. *Cell Metab.* **2017**, *25* (3), 593−609.
(3) Yan, W.; Li, R.; He, L.; Du, J.; Hou, J. *Cell. Signalling* **2015**, *27*, 851−859.
(4) Walsh, C. T.; Garneau-Tsodikova, S.; Gatto, G. J. *Angew. Chem., Int. Ed.* **2005**, *44*, 7342−7372.
(5) Hentschel, A.; Zahedi, R. P.; Ahrends, R. *Proteomics* **2016**, *16*, 759−782.
(6) Berndt, N.; Hamilton, A. D.; Sebti, S. M. *Nat. Rev. Cancer* **2011**, *11*, 775−791.
(7) Casey, P. J. *Science* **1995**, *268*, 221−225.
(8) Triola, G. *J. Glycomics Lipidomics* **2011**, S2:001.
(9) Zhang, F. L.; Casey, P. J. *Annu. Rev. Biochem.* **1996**, *65*, 241−269.
(10) Hentschel, A.; Zahedi, R. P.; Ahrends, R. *Proteomics* **2016**, *16*, 759−782.
(11) Martin, D. D.; Beauchamp, E.; Berthiaume, L. G. *Biochimie* **2011**, *93*, 18−31.
(12) Linder, M. E.; Deschenes, R. J. *Nat. Rev. Mol. Cell Biol.* **2007**, *8*, 74−84.
(13) Paulick, M. G.; Bertozzi, C. R. *Biochemistry* **2008**, *47*, 6991−7000.
(14) Benetka, W.; Koranda, M.; Eisenhaber, F. *Monatsh. Chem.* **2006**, *137*, 1241−1281.
(15) Guan, X.; Fierke, C. A. *Sci. China: Chem.* **2011**, *54*, 1888−1897.
(16) Wang, M.; Casey, P. *Nat. Rev. Mol. Cell Biol.* **2016**, *17*, 110−122.
(17) Hang, H. C.; Geutjes, E. J.; Grotenbreg, G.; Pollington, A. M.; Bijlmakers, M. J.; Ploegh, H. L. *J. Am. Chem. Soc.* **2007**, *129*, 2744−2745.
(18) Drisdel, R. C.; Green, W. N. *BioTechniques.* **2004**, *36*, 276−285.
(19) Martin, D. D.; Vilas, G. L.; Prescher, J. A.; Rajaiah, G.; Falck, J. R.; Bertozzi, C. R.; Berthiaume, L. G. *FASEB J.* **2008**, *22*, 797−806.
(20) Heal, W. P.; Wickramasinghe, S. R.; Leatherbarrow, R. J.; Tate, E. W. *Org. Biomol. Chem.* **2008**, *6*, 2308−2315.

DOI: 10.1021/acs.analchem.7b03846
Anal. Chem. 2017, 89, 13502−13507

(21) Yap, M. C.; Kostiuk, M. A.; Martin, D. D.; Perinpanayagam, M. A.; Hak, P. G.; Siddam, A.; Majjigapu, J. R.; Rajaiah, G.; Keller, B. O.; Prescher, J. A.; et al. *J. Lipid Res.* **2010**, *51*, 1566−1580.
(22) Bowman, S. M.; Piwowar, A.; Al Dabbous, M.; Vierula, J.; Free, S. J. *Eukaryotic Cell* **2006**, *5*, 587−600.
(23) Benetka, W.; Koranda, M.; Maurer-Stroh, S.; Pittner, F.; Eisenhaber, F. *BMC Biochem.* **2006**, *7*, 6.
(24) Suazo, K. F.; Schaber, C.; Palsuledesai, C. C.; Odom John, A. R.; Distefano, M. D. *Sci. Rep.* **2016**, *6*, 38615.
(25) Flynn, S. C.; Lindgren, D. E.; Hougland, J. L. *ChemBioChem* **2014**, *15*, 2205−2210.
(26) Palsuledesai, C. C.; Ochocki, J. D.; Kuhns, M. M.; Wang, Y. C.; Warmka, J. K.; Chernick, D. S.; Wattenberg, E. V.; Li, L.; Arriaga, E. A.; Distefano, M. D. *ACS Chem. Biol.* **2016**, *11*, 2820−2828.
(27) Kho, Y.; Kim, S. C.; Jiang, C.; Barma, D.; Kwon, S. W.; Cheng, J.; Jaunbergs, J.; Weinbaum, C.; Tamanoi, F.; Falck, J.; Zhao, Y. *Proc. Natl. Acad. Sci. U. S. A.* **2004**, *101*, 12479−12484.
(28) Wang, Y. C.; Dozier, J. K.; Beese, L. S.; Distefano, M. D. *ACS Chem. Biol.* **2014**, *9*, 1726−1735.
(29) Drisdel, R. C.; Alexander, J. K.; Sayeed, A.; Green, W. N. *Methods* **2006**, *40*, 127−134.
(30) Hoffman, M. D.; Kast, J. *J. Mass Spectrom.* **2006**, *41*, 229−241.
(31) Charron, G.; Zhang, M. M.; Yount, J. S.; Wilson, J.; Raghavan, A. S.; Shamir, E.; Hang, H. C. *J. Am. Chem. Soc.* **2009**, *131*, 4967−4975.
(32) Bologna, G.; Yvon, C.; Duvaud, S.; Veuthey, A. L. *Proteomics* **2004**, *4*, 1626−1632.
(33) Omaetxebarria, M. J.; Elortza, F.; Rodríguez-Suárez, E.; Aloria, K.; Arizmendi, J. M.; Jensen, O. N.; Matthiesen, R. *Proteomics* **2007**, *7*, 1951−1960.
(34) Zacharias, D. A.; Violin, J. D.; Newton, A. C.; Tsien, R. Y. *Science* **2002**, *296*, 913−916.
(35) Calero, M.; Chen, C. Z.; Zhu, W.; Winand, N.; Havas, K. A.; Gilbert, P. M.; Burd, C. G.; Collins, R. N. *Mol. Biol. Cell* **2003**, *14*, 1852−1867.
(36) Choy, E.; Chiu, V. K.; Silletti, J.; Feoktistov, M.; Morimoto, T.; Michaelson, D.; Ivanov, I. E.; Philips, M. R. *Cell* **1999**, *98*, 69−80.
(37) Roberts, P. J.; Mitin, N.; Keller, P. J.; Chenette, E. J.; Madigan, J. P.; Currin, R. O.; Cox, A. D.; Wilson, O.; Kirschmeier, P.; Der, C. *J. Biol. Chem.* **2008**, *283*, 25150−25163.
(38) Chiu, V. K.; Bivona, T.; Hach, A.; Sajous, J. B.; Silletti, J.; Wiener, H.; Johnson, R. L.; Cox, A. D.; Philips, M. R. *Nat. Cell Biol.* **2002**, *4*, 343−350.
(39) Gentry, L. R.; Nishimura, A.; Cox, A. D.; Martin, T. D.; Tsygankov, D.; Nishida, M.; Elston, T. C.; Der, C. J. *J. Biol. Chem.* **2015**, *290*, 22851−22861.
(40) Bergo, M. O.; Leung, G. K.; Ambroziak, P.; Otto, J. C.; Casey, P. J.; Young, S. G. *J. Biol. Chem.* **2000**, *275*, 17605−17610.
(41) Chen, Z.; Otto, J. C.; Bergo, M. O.; Young, S. G.; Casey, P. J. *J. Biol. Chem.* **2000**, *275*, 41251−41257.
(42) Galievsky, V. A.; Stasheuski, A. S.; Krylov, S. N. *Anal. Chem.* **2015**, *87*, 157−171.
(43) Blom, M. T.; Chmela, E.; Oosterbroek, R. E.; Tijssen, R.; Van Den Berg, A. *Anal. Chem.* **2003**, *75*, 6761−6768.
(44) Cao, S.; Pollastrini, J.; Jiang, Y. *Curr. Pharm. Biotechnol.* **2009**, *10*, 382−390.
(45) Zhang, L.; Krylov, S. N.; Hu, S.; Dovichi, N. J. *J. Chromatogr. A* **2000**, *894*, 129−134.
(46) Wang, Z.; Luo, G.; Chen, J.; Xiao, S.; Wang, Y. *Electrophoresis* **2003**, *24*, 4181−4188.
(47) Berezovski, M.; Li, W. P.; Poulter, C. D.; Krylov, S. N. *Electrophoresis* **2002**, *23*, 3398−3403.
(48) Ochocki, J. D.; Igbavboa, U.; Wood, W. G.; Arriaga, E. A.; Wattenberg, E. V.; Distefano, M. D. *Methods Mol. Biol.* **2014**, *1088*, 213−223.
(49) Hougland, J. L.; Gangopadhyay, S. A.; Fierke, C. A. *J. Biol. Chem.* **2012**, *287*, 38090−38100.
(50) Gangopadhyay, S. A.; Losito, E. L.; Hougland, J. L. *Biochemistry* **2014**, *53*, 434−446.
(51) Hartman, H. L.; Bowers, K. E.; Fierke, C. A. *J. Biol. Chem.* **2004**, *279*, 30546−30553.
(52) Cavazza, A.; Corradini, C.; Lauria, A.; Nicoletti, I.; et al. *J. Agric. Food Chem.* **2000**, *48*, 3324−3329.
(53) Reid, T. S.; Beese, L. S. *Biochemistry* **2004**, *43*, 6877−6884.
(54) End, D. W.; Smets, G.; Todd, A. V.; Applegate, T. L.; Fuery, C. J.; Angibaud, P.; Venet, M.; Sanz, G.; Poignet, H.; Skrzat, S.; et al. *Cancer Res.* **2001**, *61*, 131−137.
(55) Freed-Pastor, W. A.; Mizuno, H.; Zhao, X.; Langerød, A.; Moon, S. H.; Rodriguez-Barrueco, R.; Barsotti, A.; Chicas, A.; Li, W.; Polotskaia, A.; Bissell, M. J.; et al. *Cell* **2012**, *148*, 244−258.
(56) Hildebrandt, E. R.; Cheng, M.; Zhao, P.; Kim, J. H.; Wells, L.; Schmidt, W. K. *eLife* **2016**, *5*, e15899.
(57) Na, D. H.; Park, M. O.; Choi, S. Y.; Kim, Y. S.; Lee, S. S.; Yoo, S. D.; Lee, H. S.; Lee, K. C. *J. Chromatogr., Biomed. Appl.* **2001**, *754*, 259−263.
(58) Amon, S.; Zamfir, A. D.; Rizzi, A. *Electrophoresis* **2008**, *29*, 2485−2507.
(59) Feng, J.; Arriaga, E. A. *Electrophoresis* **2008**, *29*, 475−482.
(60) Cao, P.; Stults, J. T. *Rapid Commun. Mass Spectrom.* **2000**, *14*, 1600−1606.

DOI: 10.1021/acs.analchem.7b03846
Anal. Chem. 2017, 89, 13502−13507

Supporting Information for

Simultaneous analysis of protein expression and lipidation: a tool to study the role of protein lipidation in intracellular transduction of internal and external signals

Agnesa Shala-Lawrence,[†#] Melanie J. Blanden,[‡#] Svetlana M. Krylova,[†] Soumyashree A. Gangopadhyay,[‡] Stanislav S. Beloborodov,[†] James L. Hougland,*[‡] and Sergey N. Krylov*[,†]

[†]Department of Chemistry and Centre for Research on Biomolecular Interactions, York University, Toronto, Ontario M3J 1P3, Canada.

[‡]Department of Chemistry, Syracuse University, Syracuse, New York 13244, United States.

[#]Equal contributions

E-mail: skrylov@yorku.ca; hougland@syr.edu

Table of Contents

Experimental Procedures

Design of pJExpress414 plasmid containing His_6-eGFP-GCVDS or His_6-eGFP-GCVLL

For the eGFP-GCVDS reporter protein, site directed mutagenesis of the plasmid pJExpress_eGFP-GCVIA[1] was used to prepare an eGFP reporter protein with a C-terminal -GCVDS sequence. PCR reactions contained final concentrations of 1× Pfu Turbo buffer, 10 mM dNTPs, reverse primer (125 ng), forward primer (125 ng), template plasmid (10 ng), and Pfu Turbo DNA polymerase (1 µL, 2.5 U/µL). PCR mutagenesis was performed under the following thermal program: Initial denaturation (95°C, 1 min.); eighteen cycles of denaturation (95°C, 50 s), annealing (60°C, 50 s), and extension (68°C, 12 min); final extension (68°C, 12 min); and a final hold (10°C, ∞). The reaction was then digested with *DpnI* (1 µL, 10 U/µL) for 1 h at 37°C.

PCR mutagenesis reactions were transformed into chemically competent *E.coli* for plasmid isolation using the Z-competent transformation system (Zymo Research). An aliquot of the PCR reaction (5 µL) was added to DH5α cells (50 µL) and incubated on ice for 30 min before plating cells on warm LB-Amp plates. Cells were incubated overnight at 37°C. Colonies were chosen from the LB-Amp plate and inoculated into separate 5 mL culture of LB media with ampicillin (final concentration 100 µg/mL). Cultures were incubated overnight at 37°C with shaking. The plasmid DNA was then purified using BIO Basic Inc. EZ-10 Spin Column Plasmid DNA Minipreps Kit following the manufacturer's protocol. Mutations were verified by commercial DNA sequencing (Genewiz).

The gene for the His_6-eGFP-GCVLL reporter protein was prepared by above protocol using appropriately designed mutagenic primers. Mutations were verified by commercial DNA sequencing (Genewiz).

Creation of pCDF-Duet-1 plasmid containing the His_6-TagRFP-GCVDS reporter protein

A gene encoding the His_6-TagRFP-GCDVS reporter protein was prepared by PCR using the TagRFP-N vector[2] (Evrogen) as template with the –GCVDS C-terminal sequence and *Hind*III restriction site present in the 3' primer. The PCR reaction (50 µL) contained final concentrations of 1x Standard OneTaq buffer, 10 mM dNTPs, reverse primer (125 ng), forward primer (125 ng), template plasmid (10 ng), and OneTaq DNA polymerase (0.25 µL, 5 U/µL). PCR was performed

under the following conditions: Initial denaturation (94°C, 1 min); thirty cycles of denaturation (94°C, 30 s), annealing (56°C, 1 min), and extension (68°C, 2 min); final extension (68°C, 5 min); and a final hold (10°C, ∞). PCR products were purified using BIO Basic Inc. EZ-10 Spin Column PCR Purification Kit following the manufacturer's instructions. Following digestion by *Eco*RI and *Hind*III, the His_6-TagRFP-GCDVS insert was ligated into the pCDF-Duet-1 expression plasmid. Insert ligation was verified by analytical restriction digest and DNA sequencing (Genewiz).

Expression and purification of RL FTase and GGTase-I

Wild-type (WT) rat GGTase-I and W102R W106L rat FTase variants were expressed in BL21(DE3) *Escherichia coli* (*E. coli*) employing previously described pET23a-based GGTase-I and variant FTase vectors, with expression and purification using previously reported protocols with the following changes to protein expression.[3-5] Initial cultures were added to 1 L rich media (20 g tryptone, 10 g yeast extract, 5 g NaCl, 1% glucose, 0.5 mM IPTG and 100 µg/mL ampicillin) and grown at 28°C with shaking for 18 hours. Upon purification, enzyme concentration was measured by active-site titration using dansylated peptides, as described previously.[6]

Expression and purification of His_6-eGFP-GCVxx and His_6-TagRFP-GCVDS proteins

Chemically competent BL21 (DE3) *E. coli* were transformed with reporter protein expression vectors (pJExpress414-eGFP-GCVDS, pJExpress414-GCVLL, or CDF-Duet-1_TagRFP-GCVDS). Following transformation and antibiotic selection, a colony from the transformation plate was inoculated into LB media (5 mL) containing either 100 µg/mL ampicillin (for pJExpress414 vectors) or 100 µg/mL streptomycin (for CDF-Duet-1 vector). Cultures were incubated and shaken at 225 rpm for 4 h at 37°C. Each culture was then transferred to 1 liter of prewarmed auto-induction media (10 g tryptone, 5 g yeast extract, 20 mL 50× 5052 media [25% glycerol, 10% lactose, 2.5% glucose], 25 mM Na_2HPO_4, 25 mM KH_2PO_4, 50 mM NH_4Cl, 5 mM Na_2SO_4, 2 mM $MgSO_4$, 200 µL trace metals [50 µM $FeCl_2$, 20 µM $CaCl_2$, 10 µM $MnCl_2$, 10 µM $ZnCl_2$], 100 µg/mL ampicillin or streptomycin.[7] Expression cultures were incubated for 19 h at 37˚C with shaking. Cells were harvested by centrifugation and resuspended in 50 mL resuspension buffer (20 mM NaH_2PO_4, 500 mM NaCl, and 10 mM imidazole). Bacterial cell suspensions were lysed by sonication, clarified by centrifugation, and purified by affinity chromatography using a Ni-NTA HisTrap column (GE

Healthcare). Fractions containing the fluorescent protein were combined and concentrated using a centrifugal concentrator. Concentrated samples were buffer exchanged to 50 mM Tris buffer (pH 7.5), divided into 20 µL aliquots, and flash frozen with liquid nitrogen for storage at −80°C. Protein concentrations were determined using molar absorptivities of eGFP at 488 nm of $\varepsilon_{488} = 55{,}000$ $M^{-1}cm^{-1}$ and of TagRFP at 555 nm of $\varepsilon_{555} = 100{,}000$ $M^{-1}cm^{-1}$, respectively.[1, 2]

Farnesylation of purified His_6-eGFP-GCVDS and His_6-TagRFP-GCVDS proteins

Farnesylation of purified fluorescent proteins was performed by incubation of the appropriate substrate protein (His_6-eGFP-GCVDS or His_6-TagRFP-GCVDS, 2.5 µM) with 200 nM FTase, 10 µM of Farnesyl pyrophosphate (FPP), and 5 mM $MgCl_2$ in reaction buffer (50 mM NaHEPPSO, 5 mM TCEP, pH 7.8) in a final volume of 0.5 mL. Substrate proteins were incubated in reaction buffer for 20 min prior to reaction initiation by addition of FTase and FPP to reduce disulfide bonds. Reactions were covered with foil and incubated overnight at room temperature.

Geranylgeranylation of purified His_6-eGFP-GCVLL

Geranylgeranylation of purified His_6-eGFP-GCVLL fluorescent proteins was performed $MgCl_2$ in reaction buffer (50 mM NaHEPPSO, 5 mM TCEP, pH 7.8) in a final volume of 0.5 mL. The substrate protein was incubated in reaction buffer for 20 min prior to reaction initiation by addition of GGTase-I and Geranylgeranyl pyrophosphate (GGPP) to reduce disulfide bonds. Reactions were covered with foil and incubated overnight at room temperature.

Farnesylation of His_6-eGFP-GCVDS in bacterial lysates

A frozen 1 mL aliquot of BL21 (DE3) cells expressing His_6-eGFP-GCVDS was thawed on ice. Bacterial cells in suspension (900 mL) were lysed by addition of 100 mL of Fast Break lysis reagent (Promega) followed by moderate shaking for 15 min at room temperature. The resulting lysate was clarified by centrifugation (1,000 × *g*, 5 min). The concentration of the His_6-eGFP-GCVDS in the clarified lysate was determined by absorbance of eGFP at 488 nm of $\varepsilon_{488} = 55{,}000$ $M^{-1}cm^{-1}$).[3] Farnesylation of His_6-eGFP-GCVDS in crude lysate was performed by incubation of sufficient lysate supernatant to reach a final concentration of 2.5 µM protein with 200 nM RL

FTase, 10 μM FPP, 5 mM $MgCl_2$, reaction buffer (50 mM NaHEPPSO, 5 mM TCEP, pH 7.8) in a final volume of 0.5 mL. Supernatant containing the protein was incubated with 1× reaction buffer for 20 min to reduce disulfide bonds prior to initiation of the reaction. Reactions were incubated for overnight at room temperature.

Preparation of HEK293 cells expressing eGFP-HRas

The mammalian cell line HEK293 (ATCC) was maintained in 75 mL vented tissue culture flasks (Celltreat), and were split upon reaching 80% confluency. The cells were grown in complete DMEM (Dulbecco's Modified Eagle's Medium supplemented with 10% fetal bovine serum (FBS) and 1% (v/v) penicillin-streptomycin (MediaTech)) in a humidified atmosphere with 5% CO_2 at 37°C. For expression of the eGFP-HRas reporter protein, 9×10^4 cells were placed in 2 mL of complete DMEM per well of a tissue culture treated 6-well plate (Corning) (total of 5 wells). The cells were incubated 18-20 hours prior to transfection. The DNA-transfection reagent complex was prepared by incubating 4 μg of the reporter protein expression plasmid pEGFP-HRas (Casey laboratory, Duke University) and 9 μL of the Turbofect transfection reagent (Thermo Scientific) in a total volume of 500 μL supplement free DMEM for 15 minutes at room temperature.[8] The cells were then transfected with the prepared DNA-transfection reagent complex by drop wise addition into the wells of a 6-well tissue culture plate. A parallel set of wells was treated with the FTase inhibitor tipifarnib at a concentration of 500 nM. Following transfection for 24 h, live cells were imaged using a Zeiss Axio Vert.A1 inverted fluorescence microscope with a 470/40 nm excitation filter, a 495 nm beam splitter and a 525/50 nm emission filter to verify fluorescent protein expression and analyze fluorescence localization behavior in presence and absence of tipifarnib. The cells were then scraped and resuspended in phosphate buffered saline (PBS) followed by centrifugation to harvest the cell pellet. The cell pellets were stored at −80°C.

Creation of pCAF mammalian expression plasmid containing the Tag RFP-link(HRas)-CVLL reporter protein

A gene encoding the Tag RFP-link(HRas)-CVLL reporter protein was prepared by PCR mutagenesis by mutating the terminal serine residue of the previously reported TagRFP-link(HRas)-CVLS reporter protein to a leucine residue to obtain the pCAF1-TagRFP-link(HRas)-

CVLL vector.[9] In the Tag RFP-link(HRas)-CVLL reporter protein, the 15 amino acids of HRas upstream of the farnesylation site within Hras and a C-terminal -GCVLL sequence are fused to TagRFP (-KLNPPDESGPGCMSCGCVLL). Primers were dissolved in ultra-pure water and concentrations were measured by UV absorbance at 260 nm (1 OD = 33 µg/mL). The PCR mutagenesis reaction (50 µL) contained 10 x Pfu reaction buffer (5 µL), pCAF1-TagRFP-link(HRas)-CVLS template plasmid (10 ng), forward primer (125 ng), reverse primer (125 ng), 10 mM dNTPs, and Pfu Turbo DNA polymerase (1 µL, 2.5 U/µL). PCR mutagenesis was performed using the following temperature program: Initial denaturation (95°C, 1 min); 18 cycles of denaturation (95°C, 50 sec); annealing (60°C, 50 sec) and extension (68°C, 12 min) followed by final extension (68°C, 12 min). Following PCR, reactions were treated with DpnI (1 µL, 10 units/µL) and incubated at 37°C for 1 hour. Z-competent DH5α E. coli cells (Zymo Research) were thawed on ice for 10 minutes and then transformed with 5 µL of the PCR reaction following which the cells were plated on pre-warmed LB-Amp plates and incubated overnight at 37°C. Two colonies were picked from each plate and inoculated into LB media (5 mL) containing 100 µg/mL ampicillin and incubated with shaking (225 rpm) overnight at 37°C. Following overnight growth, a 10% glycerol stock was prepared stored at -80°C. Plasmid DNA was purified from the remaining saturated culture using EZ-10 spin column DNA purification kit (BioBasic) per the manufacturer's protocol. The mutations were confirmed by DNA sequencing (Genscript).

Preparation of MDA-231shp53 cells expressing Tag RFP-link(HRas)-CVLL in the presence and absence of doxycycline

The mammalian cell line MDA-231shp53 (CUNY-Hunter College, New York) was maintained in 75 mL vented tissue culture flasks (Celltreat), and were split upon reaching 80% confluency.[10] The cells were grown in complete DMEM in a humidified atmosphere with 5% CO_2 at 37°C. For doxycycline treatment, doxycycline (6 µg/mL) was added to the 75 mL culture flask and the cells were incubated as described above. The cells were grown in the presence of doxycycline for at least 8 days to ensure suppression of mutant p53 expression. For expression of the reporter protein, 1×10^5 cells were placed in 2 mL of complete DMEM per well (5 total wells) of a tissue culture treated 6-well plate (Corning). For the doxycycline treated cells, 6 µg/mL doxycycline was added to each well prior to transfection. Both doxycycline treated and untreated cells were incubated 18-20 h prior to transfection. The DNA-transfection reagent complex was prepared by incubating 1 µg

of the pCAF1-TagRFP-link(Hras)-CVLL reporter protein plasmid and 2 µL of the XtremeGENE HP transfection reagent (Roche) in a total volume of 100 µL supplement free DMEM for 30 min at room temperature. The cells were then transfected with the prepared DNA-transfection reagent complex by drop wise addition into the wells of a 6-well tissue culture plate. Upon 24 h transfection, live cells were imaged using a Zeiss Axio Vert.A1 inverted fluorescence microscope with a 545/525 nm excitation filter, a 565 nm beam splitter, and a 605/70 nm emission filter to verify fluorescent protein expression. The cells were then scraped and resuspended in PBS, followed by centrifugation to harvest the cell pellet. The cell pellets were stored at −80°C.

Control experiments with HEK293 cells expressing TagRFP-link(HRas)-CVLL

The mammalian cell line HEK293 (ATCC) was maintained in 75 mL vented tissue culture flasks (Celltreat), and were split upon reaching 80% confluency. The cells were grown in complete DMEM penicillin-streptomycin (MediaTech)) an in a humidified atmosphere with 5% CO_2 at 37°C. For expression of the reporter protein, 1×10^5 cells were placed in 2 mL of complete DMEM per well of a tissue culture treated 6-well plate (Corning) (5 total wells). For the doxycycline treated cells, 6 µg/mL doxycycline was added to each well prior to transfection. Both doxycycline treated and untreated cells were incubated 18-20 h prior to transfection. The DNA-transfection reagent complex was prepared by incubating 4 µg of the pCAF1-TagRFP-link(Hras)-CVLL reporter protein plasmid and 9 µL of the Turbofect transfection reagent (Thermo Scientific) in a total volume of 500 µL supplement free DMEM for 15 min at room temperature. The cells were then transfected with the prepared DNA-transfection reagent complex by drop wise addition into the wells of a 6-well tissue culture plate. Upon 24 h transfection, live cells were imaged using a Zeiss Axio Vert.A1 inverted fluorescence microscope with a 545/525 nm excitation filter, a 565 nm beam splitter and a 605/70 nm emission filter to verify fluorescent protein expression. The cells were then scraped and resuspended in PBS followed by centrifugation to harvest the cell pellet. The cell pellets were stored at −80°C.

Western blot for detection of mutant p53 expression in MDA-231shp53 cells

The doxycycline treated and untreated MDA-231shp53 cells (1×10^6 cells) were harvested and lysed. The proteins were then resolved by a 12% SDS-PAGE (150 V, 2 h) with a protein standard

(PAGE Ruler pre-stained protein ladder, Thermo Scientific). Following electrophoresis, the proteins were transferred to a polyvinylidene fluoride membrane (0.2 µm PVDF, Trans-Blot Turbo Transfer Pack, BioRad) using the Trans-Blot Turbo transfer system (25 V, 30 min followed by 1.3-25 V, 10 min) p53 was detected by using p53 antibody (sc-98, mouse monoclonal IgG1, Santa Cruz Biotechnology), as the primary antibody at a dilution of 1:200 followed by the secondary antibody, Goat anti mouse IgG-HRP (sc-2031, Santa Cruz Biotechnology) at 1:1,000 dilution. The horseradish peroxidase SuperSignal West Pico Chemiluminescent Substrate kit (Thermo Scientific) was used for detection of antibody binding. The membrane was then stripped using the stripping buffer (1 M Glycine, 0.05% Tween 20, pH 2.5) and detected for β-actin as a loading control using the mouse anti- β-actin-peroxidase (Sigma Aldrich) at a dilution of 1:25,000 (**Fig. S1**).

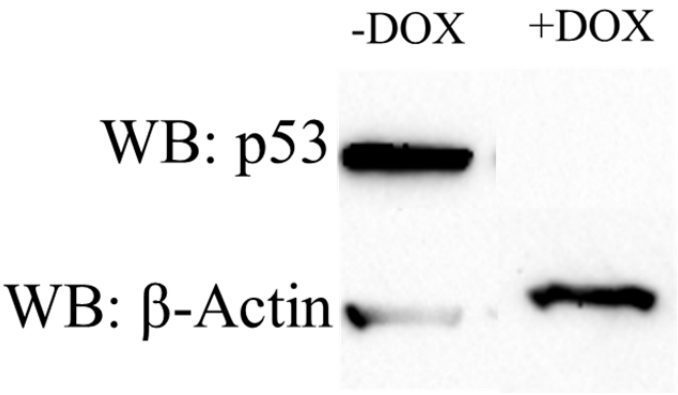

Figure S1. Doxycycline treatment of MDA-231shp53 cells suppresses mutant p53 expression. MDA-231shp53 cells express mutant p53 when not treated with doxycycline. Expression of mutant p53 (53 kDa) was suppressed in the MDA-231shp53 cells by treatment with doxycycline for > 8 days. β-Actin (42 kDa) was used as a loading control. Cells were analyzed for p53 and β-Actin expression as described in Experimental Methods.

Optimization strategy for PLQ

The following parameters were optimized to find the best separation conditions of farnesylated and non-farnesylated proteins: concentrations of SDS and borax as well as pH. To determine the optimum SDS conditions, the mixture of farnesylated and non-farnesulated eGFP were analyzed at SDS concentrations ranging from 0 to 25 mM at pH 9.2 (**Fig. S2**).

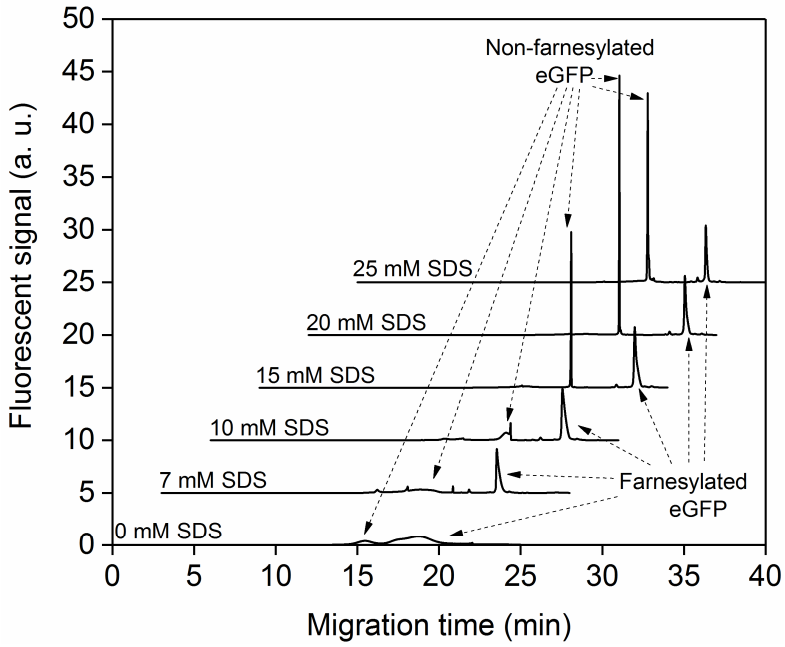

Figure S2. Influence of changing SDS concentration on separation of the farnesylated and non-farnesylated eGFP. All of the experiments were conducted in a buffer containing 25 mM borax at different concentrations of SDS (indicated on a left) and pH of 9.2. For clarity of presentation, 3-min time offsets and 5-unit signal offsets units are applied.

As follows from the **Fig. S2**, separation is poor and the proteins' peaks are merged in the absence of SDS. Separation improves with increasing concentration of SDS. The maximum resolution was achieved with SDS concentration being in a range of 15 to 25 mM; the electropherograms are reproducible and look similar to each other in this range. The same dependence was also observed for farnesylated and non-farnesylated TagRFP at pH 10.0. The slightly higher pH for TagRFP was chosen since this protein is more basic than eGFP and may require higher concentration of the hydroxide ions to be in charge conditions similar to eGFP.

Further pH optimization experiments showed that the best separation of non-farnesylated and farnesylated forms of eGFP and TagRFP could be achieved at pH 9.2 and 10.2, respectively.

Using the optimum SDS and pH conditions, we then performed a set of experiments with different borax concentrations (10, 25 and 50 mM). We found that the high borax concentration (50 mM) improves the resolution, but also causes peak broadening and unreasonably increases the migration time of the proteins, while too low concentration of borax (10 mM) makes peaks non-resolvable. The optimum separation profile for eGFP and TagRFP was obtained at the borax concentration of 25 mM, which we used throughout all our previous optimization experiment.

Estimation of the number of SDS molecules per farnesylated eGFP-GCVDS

In PLQ, electrophoretic separation of lipidated protein (P) from its non-lipidated counterpart (S) is achieved due to biding of SDS to the lipid moiety of P. Binding to the protein moiety of both S and P is possible but should not suppress the charge difference between S and P induced by SDS binding to the lipid moiety of P. Electrophoretic data can be used to roughly estimate the average number of SDS molecules bound to the lipid moiety, n, per molecule of P if we assume that, in first approximation: (i) S migrates along with electroosmotic flow and (ii) the electrophoretic mobility of S (considering the presence of the ionic atmosphere) is much smaller than that of SDS, and (iii) both S and P-(SDS)$_n$ are globular. In such a case, electrophoretic mobility of P-(SDS)$_n$ is:

$$\mu_{\mathrm{P}} = \frac{q_{\mathrm{P\text{-}(SDS)}_n}}{6\pi\eta r_{\mathrm{P\text{-}(SDS)}_n}} \approx \frac{q_{\mathrm{S}} + nq_{\mathrm{SDS}}}{6\pi\eta(r_{\mathrm{S}} + r_{\mathrm{FN}} + k^{-1})} \approx \frac{nq_{\mathrm{SDS}}}{6\pi\eta(r_{\mathrm{S}} + r_{\mathrm{FN}} + k^{-1})} \quad (1)$$

Here q denotes charge, r denotes molecular radius, η is buffer viscosity and k^{-1} is a Debye length that characterizes maximum thickness of the ionic atmosphere. The subscripts are self-explanatory, except for "FN", which denotes the farnesyl group. We assume that the radii are roughly additive, and that $r_{\mathrm{P\text{-}(SDS)}_n} = r_{\mathrm{S}} + r_{\mathrm{FN}} + k^{-1}$. The unknown that needs to be found is n.

The value of η can be assumed to be equal to that of water (~1×10^{-3} Pa·s) for dilute aqueous solutions. The value of μ_{P} can be found experimentally. The value of q_{SDS} can be assumed to be equal to the charge of the electron (-1.6×10^{-19} C) as SDS is a strong electrolyte and will exist in a solution in a fully ionized form. The values of r_{S} can be roughly estimated to be 2.1 nm based on the protein's molecular weight of 33.2 kDa in the assumption of its globular shape.[11] This value is also roughly equal to a half of protein length, since it has cylindrical structure with a length of 4.2 nm. The value of r_{FN} can be estimated in the same way and will be equal to a half of length of the farnesyl group (0.8 nm). Debye length (k^{-1}) can be found by the following formula:

$$k^{-1} = \sqrt{\frac{\varepsilon\varepsilon_0 k_{\mathrm{B}} T}{2N_{\mathrm{A}} e^2 I}} \quad (2)$$

Where ε_0 is the vacuum permittivity (8.86×10^{-12} F/m), ε is the relative permittivity of the buffer and can be assumed to be equal to that of water (78), k_{B} is Boltzmann constant (1.38×10^{-23} J/K), T is the temperature of the buffer (298 K), N_{A} is Avogadro's number (6.02×10^{-23} mol^{-1}), e is the

charge of the electron, and I is the ionic strength of the buffer (~100 mol/m^3). From eq. (2) k^{-1} is approximately equal to 1 nm.

We can now focus on finding μ_P. We will do all calculations for eGFP-GCVDS as S and farnesylated eGFP-GCVDS as P; a recorder trace of PLQ separation for these molecules is shown in **Fig. 3a** in the main text. Since we used an uncoated capillary, there was considerable EOF which should be taken into consideration. For estimating EOF mobility, μ_{EOF}, we considered S as a neutral marker that migrates with EOF (the result of one of the 3 "first-approximation" assumptions made above):

$$\mu_{EOF} = \frac{L_{det}}{t_S} \times \frac{L_{tot}}{V} \quad (3)$$

where L_{det} and L_{tot} are the distance from the capillary inlet to the detector and to the capillary outlet, respectively, t_S is the migration of S to the detector and V is the applied voltage.

The electrophoretic mobility of P can then be found as:

$$\mu_P = -\mu_{EOF} + \frac{L_{det}}{t_P} \times \frac{L_{tot}}{V} \quad (4)$$

where t_P is the migration time of P to the detector. The following experimental conditions were used: L_{tot} = 50 cm, L_{det} = 40 cm, and V = 20 kV. Experimentally determined migration times were: t_S = 5.64 and t_P = 8.24 min. By substituting these values into eqs. (3)–(4) we obtain the following values for the mobilities: $\mu_{EOF} = (1.77 \pm 0.01) \times 10^{-2}$ and $\mu_P = -(0.56 \pm 0.01) \times 10^{-2}$ cm^{2}V^{-1}min^{-1}. By using Eq. (1) we can get $n \approx 4$, which means that approximately four SDS molecules surround farnesyl fragment in P.

The previous approximation assumed that the charge of S is negligible and the protein was moving along with electroosmotic flow. However, it may not be the case. If S had a considerable charge, it would cause in non-zero electrophoretic mobility and result in a systematic error. To address this point we should find the upper and lower limits for electrophoretic mobilities of S and P (μ_{S*} and μ_{P*}, respectively) and, then, estimate the possible range of n by using eq. (1).

Since S may not be a good EOF marker, we decided to take into account previously published electropherograms of 6 different proteins with DMF as EOF marker,[12] and also electropherograms of 2 other proteins (SSB and MutS) with BODIPY as EOF marker (SSB and MutS data was obtained by us). All of the chosen proteins were analyzed in basic conditions (pH range between

8.0 and 10.0) and have isoelectric point (pI) values between 5.2-7.0, which covers pI for eGFP-GCVDS (~5.5). The electroosmotic and electrophoretic mobilities for these proteins were calculated in the same way as we did for S and P by eq. (3)-(4) and the resulting values are presented in **Table 1**. The mean value of electrophoretic mobility ($\overline{\mu}$) was found to be equal to -0.5×10^{-2} $cm^2V^{-1}min^{-1}$ with standard deviation (σ) of 0.2×10^{-2} $cm^2V^{-1}min^{-1}$. To find possible boundary conditions for μ_{S*} we treated a set of μ values with the normal distribution function and found that a range of 0 to -0.9×10^{-2} $cm^2V^{-1}min^{-1}$ covers all possible values of μ with 97% probability. It means that lower and upper limits for μ_{S*} are equal to 0 and -0.9×10^{-2} $cm^2V^{-1}min^{-1}$, respectively.

The condition of $\mu_{S*} = 0$ means that S migrates along with EOF. Such a case has already been considered above and led to $n \approx 4$ (which is the lower limit for n). The condition of $\mu_{S*} = -0.9 \times 10^{-2}$ $cm^2V^{-1}min^{-1}$ means that S migrates slower than EOF, which allows us to use the following formula to find the apparent value of μ_{EOF*}:

$$\mu_{S*} = -\mu_{EOF*} + \frac{L_{det}}{t_S} \times \frac{L_{tot}}{V} \quad (5)$$

From this equation, $\mu_{EOF*} = 2.7 \times 10^{-2}$ $cm^2V^{-1}min^{-1}$. Using this value instead of μ_{EOF} in eq. (4) allows us to find the upper limit for μ_{P*}, which is equal to -1.5×10^{-2} $cm^2V^{-1}min^{-1}$. The negative upper limit of μ_{S*} indicates that S has a considerable charge, which can be calculated from the following equation:

$$\mu_{S*} = \frac{q_{S*}}{6\pi\eta(r_S + k^{-1})} \quad (6)$$

From here, $q_{S*} = -8.8 \times 10^{-19}$ C.

Using the obtained values of μ_{p*} and q_{S*} values instead of q_S and μ_p in eq. (1) allows us to find the upper limit for n, which is equal to 6. In this case the range of possible values of n lies between 4 and 6. It is important to emphasize that this range of n is a rough estimate obtained under a set of simplifying assumptions.

Table S1. Electroosmotic (μ_0) and electrophoretic (μ) mobilities of analyzed proteins. Electroosmotic mobilities of the run buffers used and electrophoretic mobilities of proteins analyzed. Data for first 6 proteins (including pI) were found in the literature[12] and the data for MutS and SSB were obtained by us. pI values for MutS, SSB and eGFP-GCVDS were calculated by using Protein Identification and Analysis Tools on the ExPASy server.

Protein	**pI**	**Run buffer**	**Electroosmotic mobility $cm^2V^{-1}min^{-1}$**	**Electrophoretic mobility $cm^2V^{-1}min^{-1}$**
β-Globulin A	5.4	0.3 M Borax, pH 10.0	0.015	–0.006
		0.5 M Phosphate, pH 8.0	0.012	–0.007
β-Globulin B	5.2	0.3 M Borax, pH 10.0	0.015	–0.006
		0.5 M Phosphate, pH 8.0	0.012	–0.008
Conalbumin	6.6	0.3 M Borax, pH 10.0	0.015	–0.002
		0.5 M Phosphate, pH 8.0	0.012	–0.006
Myoglobin	7.0		0.012	–0.005
Carbonic anhydrase II	5.9	0.5 M Phosphate, pH 9.0	0.012	–0.004
Soybean trypsin inhibitor	4.6		0.012	–0.006
MutS	5.4	50 mM Tris-HCl, pH 8.0	0.028	–0.008
SSB	6.0		0.026	–0.005

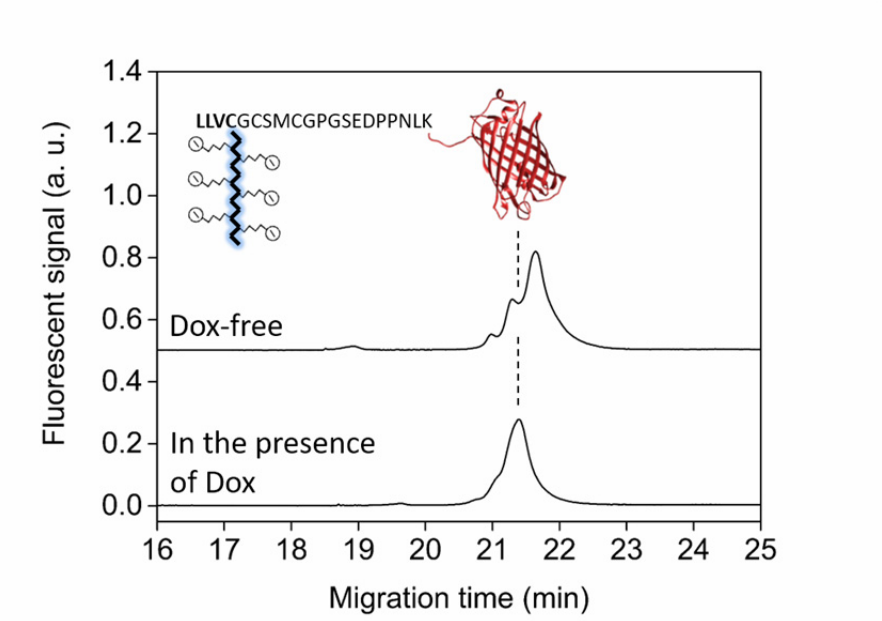

Figure S3. Control experiments with HEK293 cells in the absence of the mutated p53 gene. The upper trace shows signal of geranylgeranylated product of TagRFP-link(HRas)-CVLL expressed in HEK293 cells in the absence of doxycycline. The bottom trace shows the same peak of geranylgeranylated product expressed in HEK293 cells in the presence of doxycycline, which indicates that doxycycline treatment alone does not influence protein geranylgeranylation in the absence of the mutated p53 gene.

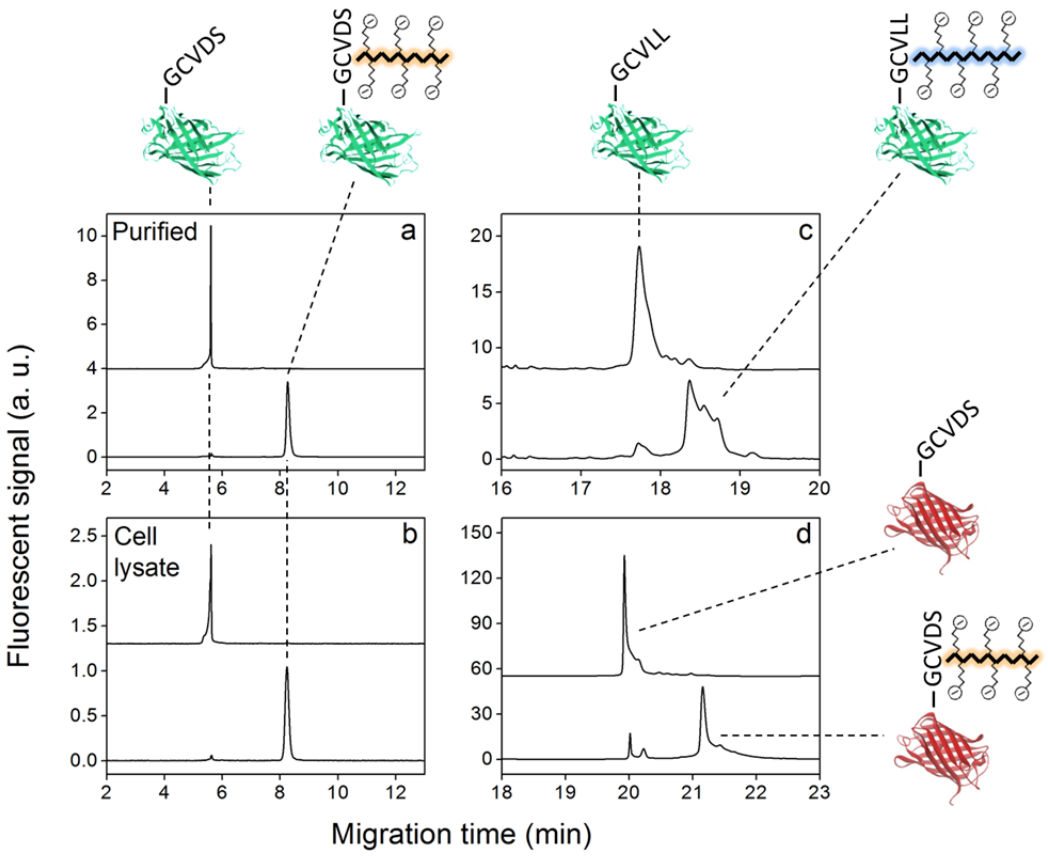

Figure S4. Representative electropherograms for the unmodified and modified proteins.

The upper line on all of the panels demonstrates the migration profile of the unmodified protein (substrate, S) and the bottom line belongs to its prenylated construct (product, P): (a) S, eGFP-GCVDS; P; farnesylated eGFP-GCVDS in 50 mM NaHEPPSO pH 7.8 and 5 mM TCEP; (b) S and P present in the crude bacterial cell lysate. The run buffer was 25 mM Borax, 20 mM SDS at pH 9.2. (c) S, eGFP-GCVLL; P, geranylgeranylated eGFP-GCVLL. Purified S and P were in 50 mM NaHEPPSO pH 7.8 and 5 mM TCEP; run buffer was 25 mM Borax, 20 mM SDS at pH 9.2 (d) S, TagRFP-GCVDS; P, farnesylated TagRFP-GCVDS. Purified S and P were in 50 mM Na-HEPPSO pH 7.8 and 5 mM TCEP; run buffer was 25 mM sodium tetraborate, 20 mM SDS at pH 10.0.

References

1. Rashidian, M.; Dozier, J. K.; Lenevich, S. & Distefano, M. D. *Chem. Comm.* **2010**, *46*(47), 8998–9000.
2. Merzlyak, E. M.; et al. *Nature Methods* **2007**, *4*, 555-557.
3. Hougland, J. L.; Gangopadhyay, S. A.; Fierke, C. A. *J. Biol. Chem.* **2012**, *45*, 38090-100.
4. Gangopadhyay, S. A.; Losito, E. L.; Hougland, J. L. *Biochemistry* **2014**, *2*, 434-46.
5. Hartman, H. L.; Bowers, K. E. and Fierke, C. A. *J. Biol. Chem*. **2004**, *279*, 30546−30553.
6. Hartman, H. L.; Hicks, K. A. and Fierke, C. A. *Biochemistry* **2005**, *44*, 15314−15324.
7. Studier, F. M. *Protein Expression & Purification* **2005**, *41*, 207-234.
8. Chen, Z.; Otto, J. C.; Bergo, M. O.; Young, S. G. and Casey, P. J. *J. Biol. Chem.* **2000**, *275*, 41251-41257.
9. Flynn, S.C.; Lindgren, D.E. and Hougland, J. L. *Chembiochem* **2014**, *15*, 2205-2210.
10. Freed-Pastor, W. A.; Mizuno, H.; Zhao, X.; Langerød, A.; Moon, S. H.; Rodriguez-Barrueco, R.; Barsotti, A.; Chicas, A.; Li, W.; Polotskaia, A.; Bissell, M. J.; Osborne, T. F.; Tian, B.; Lowe, S. W.; Silva, J. M.; Børresen-Dale, A. L.; Levine, A. J.; Bargonetti, J.; Prives, C. *Cell* **2012**, *148*, 244-58.
11. Erickson, H. P. *Biol. Proced. Online* **2009**, *11*, 32-51.
12. Chen, F-T. A.; Sternberg, G. C. *Electrophoresis* **1994**, *15*, 13-21.